

Final Report of the APMP.M.FF-S1

Final Report of the APMP Water Flow Supplementary Comparison (APMP.M.FF-S1)

Sejong Chun¹, Noriyuki Furuichi²

January 14, 2022

1 KRISS, South Korea (Pilot Lab.)

2 NMIJ, AIST, Japan (Pilot Lab.)

* APMP.M.FF-S1 is a bilateral comparison between NMIJ, AIST and KRISS.

Contents

ABSTRACT	4
LIST OF SYMBOLS.....	5
1. INTRODUCTION.....	6
2. TEST PROCEDURE.....	7
2.1. TEST PROTOCOL.....	7
2.2. FLOW CONFIGURATION.....	8
2.3. TRANSFER STANDARD.....	8
2.4. CALIBRATION PROCEDURE.....	10
2.5. TEST SCHEDULE.....	10
3. UNCERTAINTY.....	12
3.1. MATHEMATICAL MODEL.....	12
3.2.1. Repeatability for both Day #1 and Day #2.....	15
3.2.2. Reproducibility from Day #1 to Day #2.....	15
3.2.3. Re-installation effect from Day #2 to Day #3.....	16
3.2.4. Long-term stability from previous measurements to dataset #3.....	16
3.2.5. Influence of temperature change.....	18
3.2.6. Uncertainty budgets for K-factors (dataset #1).....	18
3.2.7. Inconclusiveness test for K-factors.....	20
3.3. DEFINITION OF E_n	20
4. TEST RESULTS	22
4.1. TEST RESULTS WITH THE FC ACCORDING TO CONFIGURATION #2.....	22
4.1.1. First experimental results between dataset #1 and dataset #2.....	22
4.1.2. Second experimental results between dataset #2 and dataset #3.....	23
4.2. TEST RESULTS WITHOUT THE FC ACCORDING TO CONFIGURATIONS #1 AND #3.....	24
5. CONCLUSIONS.....	27
ACKNOWLEDGEMENTS	28
REFERENCES.....	29
APPENDIX	30
A.1. TEST RESULTS BY NMIJ, AIST (DATASET #2, SEPTEMBER 11 ~ 17, 2019).....	30
A.2. TEST RESULTS BY NMIJ, AIST (CONFIGURATION #1, SEPTEMBER 11 ~ 17, 2019).....	31
A.3. TEST RESULTS BY KRISS (DATASET #1, JULY 8 ~ 12, 2019).....	32
A.4. TEST RESULTS BY KRISS (DATASET #3, NOVEMBER 24 ~ 29, 2019).....	33
A.5. TEST RESULTS BY KRISS (CONFIGURATION #3, NOVEMBER 24 ~ 29, 2019).....	34

List of Figures

Figure 1. Flow configuration of turbine flow meter and its flow conditioner for APMPM.FF-S1	7
Figure 2. Flow straightener (tube bundle) as indicated by ISO 5167-1:2003, p.23 [6].....	9
Figure 3. Transfer standards used in APMPM.FF-S1	9
Figure 4. K-factor distribution for dataset #1(Day #1 ~ #3) and dataset #3(Day Again #1 ~ #3)...	17
Figure 5. K-factor distribution for previous measurements (#1 ~ #8).....	18
Figure 6. Number of equivalence between dataset #1 (KRISS) and #2 (NMIJ, AIST).....	22
Figure 7. Test results between dataset #1 (KRISS) and #2 (NMIJ, AIST).....	23
Figure 8. Number of equivalence between dataset #2 (NMIJ, AIST) and #3 (KRISS).....	24
Figure 9. Test results between dataset #2 (NMIJ, AIST) and #3 (KRISS).....	24
Figure 10. Number of equivalence between configuration #1 (NMIJ, AIST) and #3 (KRISS)	25
Figure 11. Test results between configuration #1 (NMIJ, AIST) and #3 (KRISS)	26

List of Tables

Table 1. Specifications of transfer standards in APMPM.FF-S1	10
Table 2. Test schedule, shipping address, and contact points for APMPM.FF-S1	11
Table 3. Repeatability of dataset #1	16
Table 4. Reproducibility summarizing dataset #1 and dataset #3	16
Table 5. Re-installation effect summarizing dataset #1 and dataset #3	17
Table 6. Long-term stability from previous measurements to dataset #3	17
Table 7. Influence of temperature change during flow measurements from previous measurements to dataset #3 (Temperature change was assumed to be less than or equal to 10.1 °C.)	17
Table 8. Uncertainty budgets for K-factors from 300 m ³ /h to 1 200 m ³ /h	19
Table 9. Inconclusiveness analysis on the FM	20
Table 10. Number of equivalence between dataset #1 (KRISS) and #2 (NMIJ, AIST)	22
Table 11. Number of equivalence between dataset #2 (NMIJ, AIST) and #3 (KRISS)	23
Table 12. Number of equivalence between configuration #1 (NMIJ, AIST) and #3 (KRISS).....	25
Table 13. Relationship to the CMC's tables	27

Abstract

A supplementary comparison, entitled as APMP.M.FF-S1, has been undertaken between KRISS and NMIJ, AIST under the supervision by the Technical Committee for Fluid Flow (TCFF) in the Asia Pacific Metrology Programme (APMP). The purpose of this supplementary comparison was to prove the measurement equivalence between NMIJ, AIST and KRISS for water flow measurement standards from 300 m³/h to 1 200 m³/h. This supplementary comparison was meaningful because there has not been an international comparison for water flows greater than 300 m³/h. Previous key comparisons have been performed only from 30 m³/h to 200 m³/h [1]. Therefore, this supplementary comparison became the first inter-laboratory comparison to cover the flow range for large-capacity water flow measurement standards. In fact, the inter-laboratory comparison between NMIJ, AIST and PTB (Berlin) has been already done for such flowrate range [2], however, this inter-laboratory comparison has not been supervised by APMP or EURAMET, such that the result of inter-laboratory comparison is published in a research journal, not in the BIPM KCDB for inter-laboratory comparisons.

A turbine flow meter with the pipe diameter of 250 mm was chosen as a transfer standard in this supplementary comparison. A flow conditioner was used to define inflow conditions upstream of the turbine flow meter. The flow conditioner was a perforated plate with a well-known design. The turbine flow meter was calibrated in two ways; with or without the flow conditioner. The calibration of turbine flow meter with the flow conditioner was according to the revised test protocol for this supplementary comparison. The other calibration without the flow conditioner was performed to investigate the flow characteristics of the turbine flow meter.

K-factor was the measurand to evaluate the measurement equivalence between NMIJ, AIST and KRISS. The K-factor was corrected by considering the temperature change between the water temperature and the reference temperature of 20 °C [3]. The measurement uncertainty of the K-factor included uncertainty factors such as repeatability, day-to-day reproducibility, re-installation effect, long-term stability, and the influence by temperature change. Inconclusiveness test was also performed to see whether the K-factor was suitable for evaluating the number of equivalence between NMIJ, AIST and KRISS. The number of equivalence was found to be less than 1. The number of equivalence became better in the case without the flow conditioner than the case with the flow conditioner. The number of equivalence was found to be conclusive because the inconclusiveness index was less than 2. Therefore, the measurement equivalence between NMIJ, AIST and KRISS has been proven by this supplementary comparison.

List of symbols

E_n	Number of equivalence
K	K-factor with temperature correction [pulse/L]
K_A	K-factor without temperature correction [pulse/L]
K_{KRISS}	K-factor measured by KRISS [pulse/L]
K_{max}	Maximum K-factor [pulse/L]
K_{min}	Minimum K-factor [pulse/L]
K_{NMIJ}	K-factor measured by NMIJ, AIST [pulse/L]
K_{Nom}	Nominal K-factor of a turbine flow meter [pulse/L]
N	Number of measurements
P_{DUT}	Pulse outputs from a turbine flow meter [pulse]
T	Water temperature [°C]
$T_{@20^{\circ}\text{C}}$	Reference water temperature at 20 °C [°C]
$U(K)$	Measurement uncertainty of K [pulse/L]
V_{REF}	Reference volume by gravimetric water flow measurement standards [L]
c_i	Sensitivity Coefficient
k	Coverage factor with confidence level of about 95 %
u_A	Uncertainty due to repeatability [pulse/L]
u_{B1}	Uncertainty due to day-to-day reproducibility [pulse/L]
u_{B2}	Uncertainty due to re-installation effect [pulse/L]
u_{B3}	Uncertainty due to long-term stability [pulse/L]
u_{B4}	Uncertainty due to influence of temperature change [pulse/L]
u_{Base}	Base uncertainty [%]
u_{TS}	Uncertainty due to the transfer standard [%]
$u(K)$	Combined standard uncertainty of K [pulse/L]
α	Thermal expansion coefficient [1/K]
δK_A	Correction value due to repeatability [pulse/L]
δK_{B1}	Correction value due to day-to-day reproducibility [pulse/L]
δK_{B2}	Correction value due to re-installation effect [pulse/L]
δK_{B3}	Correction value due to long-term stability [pulse/L]
δK_{B4}	Correction value due to influence of temperature change [pulse/L]
δP_{DUT}	Correction value of the pulse outputs [pulse]
δV_{REF}	Correction value of the reference volume [L]
ν_{eff}	Effective degrees of freedom

1. Introduction

The purpose of Supplementary Comparison, APMP.M.FF-S1, was to support and to prove the calibration and measurement capability (CMC) of participating laboratories as a part of the CIPM MRA. KRISS has completed its construction of large-capacity water flow measurement standards from 10 L/h to 2 000 m³/h. After its completion of the water flow standard systems at KRISS has requested NMIJ, AIST to prove the measurement equivalence between NMIJ, AIST and KRISS by participating in a supplementary bilateral comparison. NMIJ, AIST agreed with KRISS in a condition that NMIJ, AIST and KRISS work together as co-pilot laboratories.

APMP.M.FF-S1 was named to specify that this supplementary comparison was a spin-off comparison of CCM.FF-K1 [1]. The first Key Comparison for water flow measurements was completed in 2007. The second Key Comparison started in 2015 and is still being performed under the name as CCM.FF-K1.2015. It is noticeable that APMP.M.FF-S1 has a larger flow range than the flow range used in CCM.FF-K1 and CCM.FF-K1.2015. The flow range of CCM.FF-K1 was from 30 m³/h to 200 m³/h while the flow range of APMP.M.FF-S1 was from 300 m³/h to 1 200 m³/h. A turbine flow meter with pipe diameter of 250 mm was selected as the transfer standard for APMP.M.FF-S1.

An experimental setup for the turbine flow meter became simpler, compared with the experimental setup for CCM.FF-K1 and CCM.FF-K1.2015. It was because just one flow meter was employed as the transfer standard. This experimental setup was also different from APMP.M.FF-K1, which employed just one Coriolis mass flow meter. Instead, a flow conditioner, i.e., a perforated plate, was installed upstream of the turbine flow meter to avoid unexpected inflow condition for turbine flow metering. Another inflow condition, which did not install the flow conditioner, was also tested for further investigation on the characteristics of turbine flow metering.

This report can be used as an evidence to draw concluding remarks for updating the calibration and measurement capability among the participating laboratories, according to the Guidelines for CIPM Key Comparisons [4, 5].

2. Test Procedure

2.1. Test protocol

Participating laboratories in APMP.M.FF-S1 were NMIJ, AIST (Japan) and KRISS (Korea). At the initial phase of APMP.M.FF-S1, the first version of test protocol was applied. However, the first version revealed severe problems from the KRISS side because KRISS submitted incompatible measurement results with NMIJ, AIST. After three years of research to find out the reasons for inconsistency, KRISS reported that in-house electronics, which were connected to two turbine flow meters, gave non-linear pulse output signals. Some pulses were omitted through the in-house electronic devices during flow measurements. In the meantime, flow velocity distribution within the test pipeline with the diameter of 250 mm was scrutinized by a Pitot-static tube. This affirmed that the flow velocity distribution followed the fully-developed turbulent pipe flow in the test pipelines. KRISS concluded that active pulse outputs could be a good option for inter-laboratory comparison purposes.

The second version of test protocol limited its scope for test pipelines from (250A and 400A) to (250A only). The flow range was also reduced from [200 to 2 000] m³/h to [300 to 1 200] m³/h. Specifically, the water flow measurement standards were operated at [300, 600, 900, and 1 200] m³/h with pipe diameter of 259.6 mm (250A). Extra electronics, such as in-house electronic devices, were not allowed to be used. The transfer standard was changed to another turbine flow meter with active pulse outputs instead of passive pulse outputs. Installation of a flow conditioner was mandatory to define the inflow conditions upstream of the turbine flow meter as shown in Fig. 1.

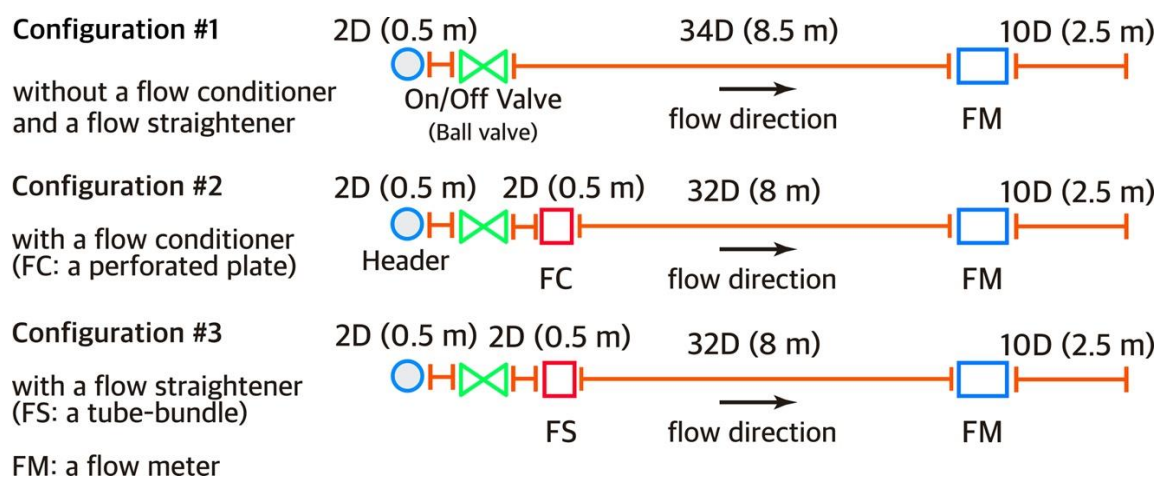


Figure 1. Flow configuration of turbine flow meter and its flow conditioner for APMP.M.FF-S1

- (a) Configuration #1: Long straight pipe length;
- (b) Configuration #2: Flow conditioner with a perforated plate (OVAL-FC);
- (c) Configuration #3: Flow straightener with a 19-tube bundle by ISO 5167-1:2003 (in-house product)

2.2. Flow configuration

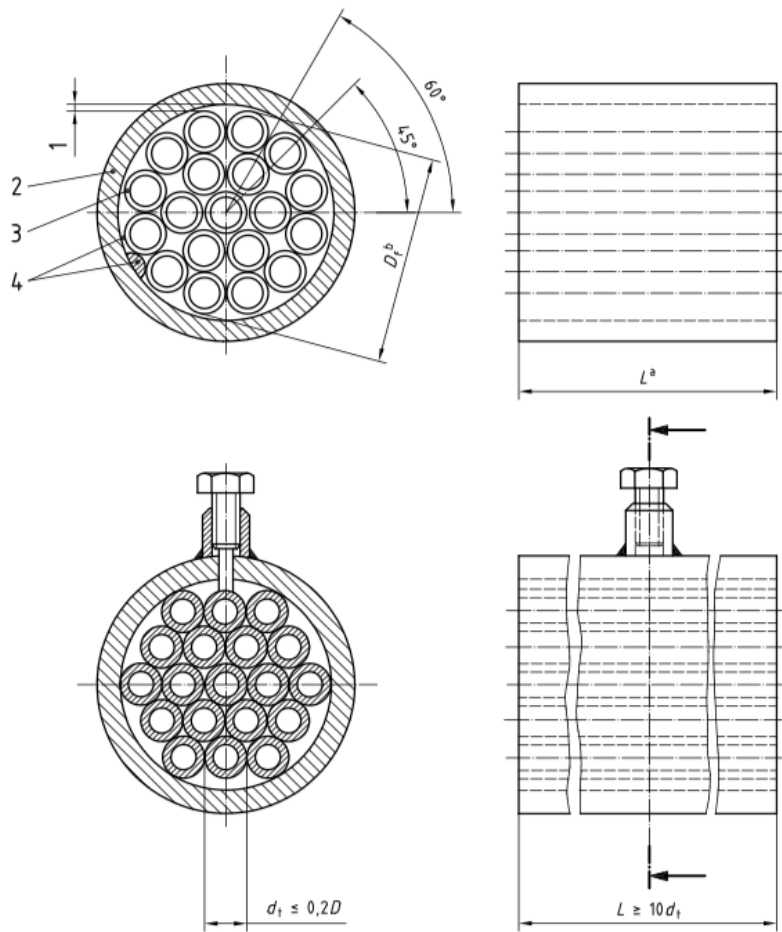
Among the three flow configurations, configuration #2 was selected for a bilateral comparison between NMIJ, AIST and KRISS. Although the configuration #2 was the default flow configuration for APMP.M.FF-S1, both configuration #1 and configuration #3 were also considered as the other bilateral comparison between NMIJ, AIST and KRISS. The configuration #1 had a very long pipeline for flow metering, such that the configuration #1 was suitable for NMIJ, AIST. The configuration #3 had a short pipeline downstream of a tube-bundle flow straightener (hereafter, FS), which was as shown in Fig. 2. This configuration was suitable for KRISS. It was because KRISS had a short pipeline for flow metering, i.e., $34D$.

The FS could shorten the upstream pipe length by suppressing flow disturbance due to valves and elbows according to ISO 5167-1 [6]. Nevertheless, the FS did not guarantee whether the asymmetric flow velocity profile could be changed into the fully-developed turbulent velocity profile by installing the FS [6]. The upstream pipe length of $34D$ as shown in Fig. 1 was not an issue. The issue was whether the fully-developed turbulent velocity profile could be established upstream of the FC. Therefore, NMIJ, AIST has agreed with KRISS to provide experimental data for the bilateral comparison between the configuration #1 (NMIJ, AIST) and the configuration #3 (KRISS).

2.3. Transfer standard

The turbine flow meter (hereafter, FM) and a flow conditioner (hereafter, FC) were specified as shown in Table 1 and Fig. 3. The FM had the nominal pipe diameter of 267.4 mm and the pipe thickness of 4.0 mm (250A 10S) according to KS D3576 and JIS G3459. 10S means that the stainless pipe can withstand pressure up to 10 bar (10 kgf/cm², gage pressure). The inner diameter of the FM was 259.4 mm. The FC was a Mitsubishi-type perforated plate with 35 holes. The FC was installed at $32D$ upstream of the FM as shown in Fig. 1 (configuration #2). Here, D means the pipe diameter.

K-factor in units of [pulse/L] was selected as the measurand for APMP.M.FF-S1. The K-factor indicated the number of pulse outputs from the FM during a certain period of time. Liquid volume was collected by a gravimetric water flow measurement standard. Elapsed time was determined by a flow diverter attached on the gravimetric water flow measurement standard. Since the K-factor was sensitive to the inflow conditions upstream of the FM, the K-factor could be used for diagnosing the performance of gravimetric water flow measurement standards.



Key

- 1 minimized gap
- 2 pipe wall
- 3 tube wall thickness (which is less than $0,025D$)
- 4 centring spacer options – typically 4 places

^a The length, L , of the tubes shall be between $2D$ and $3D$, preferably as close to $2D$ as possible.

^b D_t = flow straightener outside diameter, and $0,95D \leq D_t \leq D$.

Figure C.1 — Examples of the tube bundle flow straightener

Figure 2. Flow straightener (tube bundle) as indicated by ISO 5167-1:2003, p.23 [6]



Flow meter (side view)

(front view)

Flow conditioner

Figure 3. Transfer standards used in APMPM.FF-S1

Table 1. Specifications of transfer standards in APMP.M.FF-S1

Name	Flow Meter (FM)	Flow Conditioner (FC)
Type	Turbine flow meter	Perforated Plate for FM
Manufacturer	Oval Inc.	Oval Inc.
Model	TX1250-D11-981	Honey Vane S
S/N	T25-0150P	
Diameter	250 mm	250 mm
Weight	90.8 kg	15.6 kg
Size	400 mm x 508 mm x 527 mm	330 mm x 330 mm x 30 mm

2.4. Calibration procedure

Calibration procedure for APMP.M.FF-S1 was given as follows:

1) Day #1: flow meter calibration

A turbine flow meter (i.e., FM) was calibrated at [300, 600, 900, 1 200] m³/h with repeatable measurements of five times. For example, [1 200, 1 200, ..., 1 200] m³/h, [900, 900, ..., 900] m³/h, ... , [300, 300, ..., 300] m³/h were tested. After the flow meter calibration, FM was kept being installed. Power lines were still turned-on.

2) Day #2: flow meter calibration without remounting the flow meter

The same experiments as Day 1 were repeated. After the flow meter calibration, the power lines were turned-off. Then, FM was uninstalled from the test pipeline.

3) Day #3: flow meter calibration with remounting the flow meter

FM was remounted to the test line before another calibration. The power lines were also turned-on. The same experiments as Day #2 were repeated. After the experiment, the power lines were turned-off and FM was uninstalled.

It is noticeable that the number of pulses must be collected more than 10 000. Since the nominal K-factor was 1.961 9 pulse/L, 1 pulse could indicate 0.509 7 L. On the contrary, 10 000 pulses indicated 5 097 L. This means that the error bounds of pulse readings were less than or equal to ± 0.01 % by obtaining 10 000 pulses.

2.5. Test schedule

Test schedule, shipping address, and contact points for each participating laboratory were summarized as shown in Table 2. KRISS started a round-robin test in July 2019 by calibrating the FM according to the second version of test protocol. NMIJ, AIST participated in the round-robin test in September 2019. KRISS finished the round-robin test in November 2019 by re-calibrating the FM. The calibration data tested at KRISS were

compiled to evaluate the above-mentioned uncertainty factors before and after the round-robin test. For example, KRISS tested the FM several times from October 2018 to July 2019, before beginning the round-robin test.

Table 2. Test schedule, shipping address, and contact points for APMP.M.FF-S1

No.	Date	NMI	Address
1	July 8, 2019 July 12, 2019 (dataset #1)	KRISS (South Korea)	Korea Research Institute of Standards and Science 205-dong 101-ho, Gajeong-ro 267, Yuseong-gu Daejeon, 34113, South Korea Contact: Sejong Chun (sjchun@kriss.re.kr)
2	September 11, 2019 September 17, 2019 (dataset #2)	NMIJ, AIST (Japan)	National Metrology Institute of Japan N15a, Tsukuba North Site, AIST 1497-1 Teragu, Tsukuba, 300-4201, Japan Contact: Noriyuki Furuichi (furuichi.noriyuki@aist.go.jp)
3	November 24, 2019 November 29, 2019 (dataset #3)	KRISS (South Korea)	Korea Research Institute of Standards and Science 205-dong 101-ho, Gajeong-ro 267, Yuseong-gu Daejeon, 34113, South Korea Contact: Sejong Chun (sjchun@kriss.re.kr)

3. Uncertainty

3.1. Mathematical model

The K-factor of the transfer standard is expressed as follows.

$$K_A = \frac{P_{DUT}}{V_{REF}} \quad [\text{pulse/L}] \quad (1)$$

Here, K_A is the measured value of K-factor [pulse/L], P_{DUT} is the number of pulses of the transfer standard [pulse], and V_{REF} is the liquid volume indicated by the gravimetric water flow measurement standards [L]. The acronym REF indicates the measurement value by the gravimetric water flow measurement standard. DUT indicates the measurement value by the transfer standard, i.e., the FM.

The K-factor can be influenced by several uncertainty factors as follows.

- 1) Repeatability at each participating laboratory (u_A)
- 2) Day-to-day reproducibility from Day #1 to Day #2 (u_{B1})
- 3) Re-installation effect from Day #2 to Day #3 (u_{B2})
- 4) Long-term stability while preparing for the APMPM.FF-S1 (u_{B3})
- 5) Influence of temperature change (u_{B4})

The uncertainty factors can be incorporated into the mathematical model as follows.

$$\begin{aligned} K &= K_A \left(1 + \frac{\delta K_A}{K_A}\right) \left(1 + \frac{\delta K_{B1}}{K_A}\right) \left(1 + \frac{\delta K_{B2}}{K_A}\right) \left(1 + \frac{\delta K_{B3}}{K_A}\right) \left(1 + \frac{\delta K_{B4}}{K_A}\right) & [\text{pulse/L}] \quad (2) \\ &\cong K_A \left(1 + \frac{\delta K_A}{K_A} + \frac{\delta K_{B1}}{K_A} + \frac{\delta K_{B2}}{K_A} + \frac{\delta K_{B3}}{K_A} + \frac{\delta K_{B4}}{K_A}\right) & [\text{pulse/L}] \\ &\cong K_A + \delta K_A + \delta K_{B1} + \delta K_{B2} + \delta K_{B3} + \delta K_{B4} & [\text{pulse/L}] \end{aligned}$$

Here, δK_A is the correction value due to repeatability [pulse/L], δK_{B1} is the correction value due to day-to-day reproducibility [pulse/L], δK_{B2} is the correction value due to re-installation effect [pulse/L], δK_{B3} is the correction value due to long-term stability [pulse/L], and δK_{B4} is the correction value due to temperature change [pulse/L].

Equation (2) requires that $\delta K_A \ll K_A$, $\delta K_{B1} \ll K_A$, $\delta K_{B2} \ll K_A$, $\delta K_{B3} \ll K_A$, $\delta K_{B4} \ll K_A$. In addition, $\delta K_A = \delta K_{B1} = \delta K_{B2} = \delta K_{B3} = 0$, and $\delta K_{B4} = -3\alpha K_A \Delta T$. It is noticeable that δK_{B4} is not zero because δK_{B4} plays a role to correct K_A by temperature difference, ΔT . Then, K becomes as follows.

$$K = K_A (1 - 3\alpha \Delta T) \quad [\text{pulse/L}] \quad (3)$$

Here, α is the thermal expansion coefficient of meter body [1/K]. It is noticeable that the thermal expansion coefficient of stainless steel (SUS 304) was used in APMP.M.FF-S1. According to the literature, the thermal expansion coefficient of SUS 304 was 15.9×10^{-6} 1/K at 20 °C [7]. Its accuracy was reported better than ± 1 % [7]. Therefore, the measurement uncertainty of the thermal expansion coefficient could be estimated as 1 %, which was equivalent to 1.6×10^{-7} 1/K.

Equation (3) requires that there is thermal equilibrium between the meter body and water. If water temperature is increased, metering volume within the FM is increased by thermal expansion. On the contrary, the metering volume is decreased as the water temperature is decreased. This means that K behaves as a function of water temperature on the opposite way because the metering volume is located in the denominator of K in Eq. (1).

In evaluating K , K_A with water temperature T_{water} [°C] is corrected by the reference water temperature at 20 °C, i.e., $T_{@20^\circ\text{C}}$ [°C]. Since temperature is changed from T_{water} to $T_{@20^\circ\text{C}}$, the temperature difference is expressed as follows.

$$\Delta T = T_{@20^\circ\text{C}} - T_{\text{water}} \quad [\text{K}] \quad (4)$$

Therefore, K is also expressed as follows.

$$K = K_A (1 - 3\alpha(T_{@20^\circ\text{C}} - T_{\text{water}})) \quad [\text{pulse/L}] \quad (5)$$

3.2. Measurement uncertainty

Uncertainty of the K-factor can be evaluated as follows [8-10].

$$\begin{aligned} u(K) &= \sqrt{\frac{u^2(K_A) + u^2(\delta K_A) + u^2(\delta K_{B1})}{+u^2(\delta K_{B2}) + u^2(\delta K_{B3}) + u^2(\delta K_{B4})}} \quad [\text{pulse/L}] \quad (6) \\ &= \sqrt{\frac{c_{P_{\text{DUT}}}^2 u^2(\delta P_{\text{DUT}}) + c_{V_{\text{REF}}}^2 u^2(\delta V_{\text{REF}}) + u_A^2}{+u_{B1}^2 + u_{B2}^2 + u_{B3}^2 + u_{B4}^2}} \quad [\text{pulse/L}] \end{aligned}$$

Here, $u(K)$ is the combined standard uncertainty of K [pulse/L], $u(\delta K_A)$ is the uncertainty due to repeatability (u_A) [pulse/L], $u(\delta K_{B1})$ is the uncertainty due to reproducibility (u_{B1}) [pulse/L], $u(\delta K_{B2})$ is the uncertainty due to re-installation effect (u_{B2}) [pulse/L], $u(\delta K_{B3})$ is the uncertainty due to long-term stability (u_{B3}) [pulse/L], and $u(\delta K_{B4})$ is the uncertainty due to influence by temperature change (u_{B4}) [pulse/L].

$c_{P_{DUT}}$ and $c_{V_{REF}}$ are sensitivity coefficients as follows.

$$c_{P_{DUT}} = \frac{\partial K_A}{\partial P_{DUT}} = \frac{1}{V_{REF}} \quad [1/L] \quad (7)$$

$$c_{V_{REF}} = \frac{\partial K_A}{\partial V_{REF}} = -\frac{P_{DUT}}{V_{REF}^2} \quad [\text{pulse}/L^2] \quad (8)$$

Here, $c_{P_{DUT}}$ is the sensitivity coefficient of K_A to P_{DUT} [1/L], $c_{V_{REF}}$ is the sensitivity coefficient of K_A to V_{REF} [pulse/L²], $u(\delta P_{DUT})$ is the uncertainty due to pulse counting [pulse], and $u(\delta V_{REF})$ is the base uncertainty by the gravimetric water flow measurement standard [L].

Each uncertainty factor from δK_A to δK_{B4} can be summarized as follows. $u_A (= u(\delta K_A))$ is changed whenever K is measured on Day #1, Day #2, Day #3, etc.. For each measurement, an averaged value of K is obtained as $\overline{K_{A,\#1}}$, $\overline{K_{A,\#2}}$, $\overline{K_{A,\#3}}$, etc..

$u_{B1} (= u(\delta K_{B1}))$ is evaluated from the relationship between $\overline{K_{A,\#1}}$ and $\overline{K_{A,\#2}}$. Since K should be averaged between $\overline{K_{A,\#1}}$ and $\overline{K_{A,\#2}}$ according to the revised test protocol for APMPM.FF-S1, u_{B1} has a rectangular probability distribution at the center of $(\overline{K_{A,\#1}} + \overline{K_{A,\#2}})/2$. This means that the difference between $\overline{K_{A,\#1}}$ and $\overline{K_{A,\#2}}$ is divided by $2\sqrt{3}$.

$u_{B2} (= u(\delta K_{B2}))$ is evaluated from the relationship between $\overline{K_{A,\#2}}$ and $\overline{K_{A,\#3}}$. By the way, $\overline{K_{A,\#3}}$ is not used to evaluate K according to the revised protocol. Since u_{B2} has also a rectangular probability distribution, this means that the difference between $\overline{K_{A,\#2}}$ and $\overline{K_{A,\#3}}$ is divided by $\sqrt{3}$.

$u_{B3} (= u(\delta K_{B3}))$ is evaluated by overall trend from $\overline{K_{A,Prev.Meas.}}$ to $\overline{K_{A,\#3}}$. Since every averaged value of K should be located between upper and lower bounds of all the averaged values from $\overline{K_{A,Prev.Meas.}}$ to $\overline{K_{A,\#3}}$, u_{B3} has the rectangular probability distribution. This means that the difference between the upper and the lower bounds is divided by $2\sqrt{3}$.

$u_{B4} (= u(\delta K_{B4}))$ is evaluated from the expression $\delta K_{B4} = -3\alpha K_A \Delta T$. In this case, the temperature difference is from Day #1 to Day #3 during the round-robin test. The temperature difference at KRISS was 6.7 °C. Thus, $\Delta T \cong 10$ °C is assumed to evaluate u_{B4} . Since u_{B4} has the rectangular probability distribution, this means that $(\overline{K_{A,\#1}} + \overline{K_{A,\#2}})/2$, multiplied by $3\alpha \Delta T$, is divided by $2\sqrt{3}$. In summary, every uncertainty factor can be expressed as follows.

$$u(\delta K_A) = \sqrt{\frac{1}{N(N-1)} \sum_{i=1}^N (K_{A,i} - \overline{K_A})^2} \quad [\text{pulse}/L] \quad (9)$$

$$u(\delta K_{B1}) = \frac{|\overline{K_{A,\#2}} - \overline{K_{A,\#1}}|}{2\sqrt{3}} \quad [\text{pulse}/L] \quad (10)$$

$$u(\delta K_{B2}) = \frac{|K_{A,\#3} - K_{A,\#2}|}{\sqrt{3}} \quad [\text{pulse/L}] \quad (11)$$

$$u(\delta K_{B3}) = \frac{\max(\overline{K_{A,Prev.Meas.}}, K_{A,\#1}, K_{A,\#2}, K_{A,\#3}) - \min(\overline{K_{A,Prev.Meas.}}, K_{A,\#1}, K_{A,\#2}, K_{A,\#3})}{2\sqrt{3}} \quad [\text{pulse/L}] \quad (12)$$

$$u(\delta K_{B4}) = \frac{3\alpha\Delta T(K_{A,\#1} + K_{A,\#2})}{4\sqrt{3}} \quad [\text{pulse/L}] \quad (13)$$

Here, N is the number of data for each measurement, and $\Delta T = 10.1$ [K].

The measurement uncertainty of K is evaluated as follows.

$$U(K) = ku(K) \quad [\text{pulse/L}] \quad (14)$$

Here, k is the coverage factor with confidence level of 95 %. k is determined by the effective degrees of freedom, based on either Gaussian or Student- t distribution. The effective degrees of freedom is expressed as follows [8, 9].

$$v_{\text{eff}} = \frac{u^4(K)}{\frac{u_A^4}{N-1} + \frac{u_{B1}^4}{\infty} + \frac{u_{B2}^4}{\infty} + \frac{u_{B3}^4}{\infty} + \frac{u_{B4}^4}{\infty}} = \frac{(N-1)u^4(K)}{u_A^4} \quad (15)$$

Here, v_{eff} is the effective degrees of freedom. If v_{eff} is greater than 10, $u(K)$ is assumed to have the Gaussian probability distribution. This means that $k = 2$ with confidence level of about 95 %. If v_{eff} is smaller than or equal to 10, $u(K)$ is assumed to have the Student- t probability distribution. This means that k must be evaluated from the Student- t probability distribution with confidence level of 95 %.

3.2.1. Repeatability for both Day #1 and Day #2

K_A indicates an averaged value between $K_{A,\#1}$ and $K_{A,\#2}$. This means that $K_{A,i}$ in Eq. (9) includes both Day #1 and Day #2 data. $\overline{K_A}$ is equal to $(\overline{K_{A,\#1}} + \overline{K_{A,\#2}})/2$. If u_A is evaluated separately from 300 m³/h to 1 200 m³/h, its value can be summarized as shown in Table 3. Here, q_{REF} is the reference volume flow rate measured by the gravimetric flow measurement standard at KRISS [m³/h]. K_A is the averaged value of ten measurement data (five from Day #1, and five from Day #2) at each flow rate. u_A is the standard uncertainty based on the ten measurement data. u_A had its maximum value of 0.000 19 pulse/L at 602.65 m³/h. Its relative value amounted to 0.0096 % \cong 0.01 %.

3.2.2. Reproducibility from Day #1 to Day #2

δK_{B1} indicates difference between $K_{A,\#1}$ and $K_{A,\#2}$. Since K_A takes the averaged value between $K_{A,\#1}$ and $K_{A,\#2}$, K_A is already corrected by the amount of $\delta K_{B1}/2$. Thus, u_{B1} can be evaluated by Eq. (10) as shown in Table 4. Here, $K_{A,\#1}$ and $K_{A,\#2}$ are the K-

factors by dataset #1. $K_{A,\#1Again}$ and $K_{A,\#2Again}$ are the K-factors by dataset #3. Then, u_{B1} takes the largest value between dataset #1 and #3 at each flow rate. u_{B1} showed its maximum value of 0.000 17 pulse/L at 602.65 m³/h. The relative value was converted into 0.0087 %.

3.2.3. Re-installation effect from Day #2 to Day #3

δK_{B2} indicates difference between $K_{A,\#2}$ and $K_{A,\#3}$. Since K_A only takes the averaged value between $K_{A,\#1}$ and $K_{A,\#2}$, K_A is not corrected by δK_{B2} . Thus, u_{B2} can be evaluated by Eq. (11) as shown in Table 5. Here, $K_{A,\#2}$ and $K_{A,\#3}$ are the K-factors by dataset #1. $K_{A,\#2Again}$ and $K_{A,\#3Again}$ are the K-factors by dataset #3. Then, u_{B2} takes the largest value between dataset #1 and #3 at each flow rate. u_{B2} showed its maximum value of 0.000 39 pulse/L at 602.65 m³/h. The relative value was converted into 0.0199 % \cong 0.02 %.

3.2.4. Long-term stability from previous measurements to dataset #3

δK_{B3} indicates difference from $K_{A,Prev.Meas.}$ to $K_{A,\#3Again}$. Since K_A should be located within the minimum and the maximum bounds from $K_{A,Prev.Meas.}$ to $K_{A,\#3Again}$, u_{B3} can be evaluated by Eq. (12) as shown in Table 6. u_{B3} had its maximum value of 0.000 56 pulse/L at 602.65 m³/h. The relative value was converted into 0.028 %.

Table 3. Repeatability of dataset #1

q_{REF} [m ³ /h]	K_A [pulse/L]	$u(\delta K_A)$ [pulse/L]	$u(\delta K_A)/K_A$ [%]
1 201.44	1.964 8	0.000 06	0.0028
902.05	1.965 3	0.000 15	0.0074
602.65	1.964 1	0.000 19	0.0096
301.79	1.963 2	0.000 15	0.0077

Table 4. Reproducibility summarizing dataset #1 and dataset #3

(dataset #1: $K_{A,\#1}$, $K_{A,\#2}$; dataset #3: $K_{A,\#1Again}$, $K_{A,\#2Again}$)

q_{REF} [m ³ /h]	$K_{A,\#1}$ [pulse/L]	$K_{A,\#2}$ [pulse/L]	$K_{A,\#1Again}$ [pulse/L]	$K_{A,\#2Again}$ [pulse/L]	$u(\delta K_{B1})$ [pulse/L]	$u(\delta K_{B1})/K_A$ [%]
1 201.44	1.964 9	1.964 8	1.964 2	1.964 4	0.000 07	0.0034
902.05	1.965 1	1.965 5	1.964 1	1.963 9	0.000 13	0.0068
602.65	1.964 1	1.964 1	1.963 6	1.963 0	0.000 17	0.0087
301.79	1.963 3	1.963 1	1.963 0	1.962 9	0.000 04	0.0019

Table 5. Re-installation effect summarizing dataset #1 and dataset #3

(dataset #1: $K_{A,\#2}$, $K_{A,\#3}$; dataset #3: $K_{A,\#2\text{Again}}$, $K_{A,\#3\text{Again}}$)

q_{REF} [m ³ /h]	$K_{A,\#2}$ [pulse/L]	$K_{A,\#3}$ [pulse/L]	$K_{A,\#2\text{Again}}$ [pulse/L]	$K_{A,\#3\text{Again}}$ [pulse/L]	$u(\delta K_{B2})$ [pulse/L]	$u(\delta K_{B2})/K_A$ [%]
1 201.44	1.964 8	1.964 9	1.964 4	1.964 2	0.000 12	0.0062
902.05	1.965 5	1.965 4	1.963 9	1.964 4	0.000 32	0.0165
602.65	1.964 1	1.963 8	1.963 0	1.963 7	0.000 39	0.0199
301.79	1.963 1	1.963 2	1.962 9	1.962 6	0.000 19	0.0094

Table 6. Long-term stability from previous measurements to dataset #3

q_{REF} [m ³ /h]	K_A [pulse/L]	$u(\delta K_{B3})$ [pulse/L]	$u(\delta K_{B3})/K_A$ [%]
1 201.44	1.964 8	0.000 31	0.016
902.05	1.965 3	0.000 53	0.027
602.65	1.964 1	0.000 56	0.028
301.79	1.963 2	0.000 52	0.027

Table 7. Influence of temperature change during flow measurements from previous measurements to dataset #3 (Temperature change was assumed to be less than or equal to 10.1 °C.)

q_{REF} [m ³ /h]	K_A [pulse/L]	$u(\delta K_{B4})$ [pulse/L]	$u(\delta K_{B4})/K_A$ [%]
1 201.44	1.964 8	0.000 27	0.014
902.05	1.965 3	0.000 27	0.014
602.65	1.964 1	0.000 27	0.014
301.79	1.963 2	0.000 27	0.014

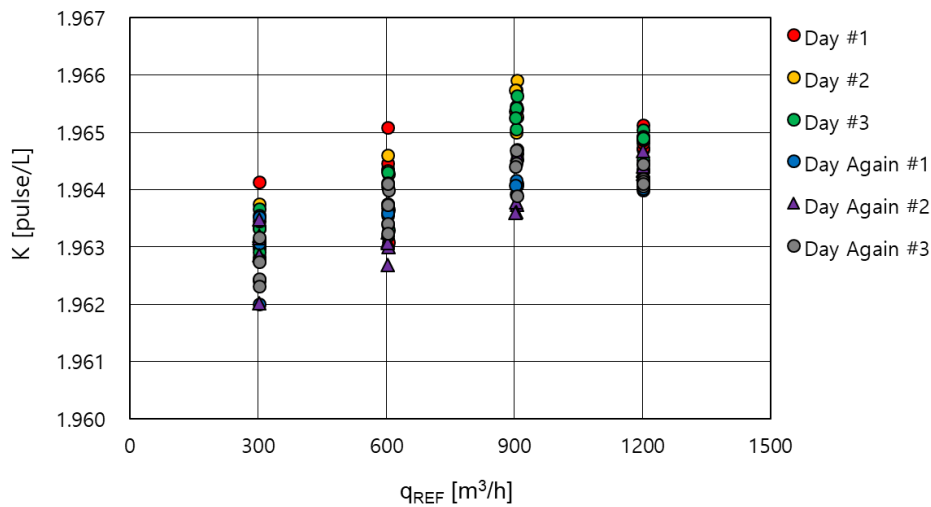


Figure 4. K-factor distribution for dataset #1(Day #1 ~ #3) and dataset #3(Day Again #1 ~ #3)

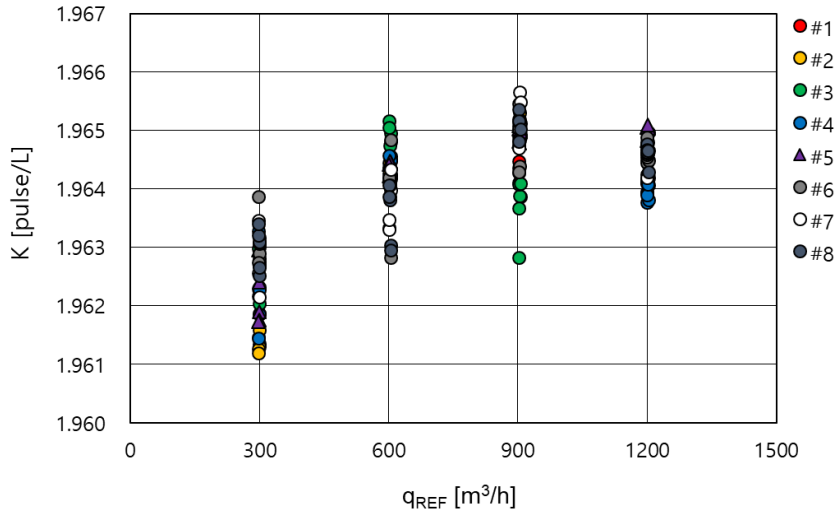


Figure 5. K-factor distribution for previous measurements (#1 ~ #8)

3.2.5. Influence of temperature change

δK_{B4} indicates the influence of temperature change during flow measurements. Based on the measured data from $K_{A,Prev.Meas.}$ to $K_{A,\#3Again}$, the minimum temperature was 14.0 °C and the maximum temperature was 24.1 °C. Thus, the temperature difference during flow measurements was 10.1 °C. Since the thermal expansion coefficient of SUS 304 stainless steel is 15.9×10^{-6} 1/K at 20 °C [7], u_{B4} can be evaluated by Eq. (13) as shown in Table 7. u_{B4} had the value of 0.000 27 pulse/L at every flow rate. Its relative value was converted into 0.014 %.

3.2.6. Uncertainty budgets for K-factors (dataset #1)

Uncertainty budgets from 300 m³/h to 1 200 m³/h can be summarized as shown in Tables 8. At $q_{REF} = 1\ 201.44$ m³/h, δV_{REF} showed the biggest influence to $u(K)$. δK_{B3} had the second biggest influence to $u(K)$. This means that the base uncertainty influenced $u(K)$ more than the long-term stability of the FM at 1 200 m³/h. However, the relationship between the base uncertainty and the long-term stability was almost the same at [300, 600, 900] m³/h.

This might mean that the inflow condition of the FM becomes better at 1 200 m³/h than at the other flow rates. This also indicates that the FC suppresses the flow disturbance better as the flow rate is increased. Either the metering performance of the FM or the flow characteristics of a flow diverter, which is attached to the gravimetric water flow measurement standard, could become an issue, otherwise.

The effective degrees of freedom exceeded 10 such that the Gaussian probability distribution was assumed to $u(K)$. Thus, the coverage factor was set to 2 with the confidence level of about 95 % for evaluating $U(K)$.

Table 8. Uncertainty budgets for K-factors from 300 m³/h to 1 200 m³/h

(a) 1 201.44 m³/h

Quantity X_j	Value x_j		Uncertainty $u(x_j)$		Prob. Dist.	Sens. Coeff. c_i		$c_i u(x_j)$		ν
δK_A	0.0E+00	pulse/L	5.6E-05	pulse/L	t	1.0E+00	-	5.6E-05	pulse/L	4
δK_{B1}	0.0E+00	pulse/L	6.7E-05	pulse/L	rectangular	1.0E+00	-	6.7E-05	pulse/L	∞
δK_{B2}	0.0E+00	pulse/L	1.2E-04	pulse/L	rectangular	1.0E+00	-	1.2E-04	pulse/L	∞
δK_{B3}	0.0E+00	pulse/L	3.1E-04	pulse/L	rectangular	1.0E+00	-	3.1E-04	pulse/L	∞
δK_{B4}	0.0E+00	pulse/L	2.7E-04	pulse/L	rectangular	1.0E+00	-	2.7E-04	pulse/L	∞
δP_{DUT}	4.1E+04	pulse	4.1E-01	pulse	rectangular	4.8E-05	1/L	1.9E-05	pulse/L	∞
δV_{REF}	2.1E+04	L	6.3E+00	L	rectangular	-9.3E-05	pulse/L ²	-5.9E-04	pulse/L	∞
K_A	1.964 6	pulse/L						7.4E-04	pulse/L	121 338
$U(K)$								1.5E-03	pulse/L	

(b) 902.05 m³/h

Quantity X_j	Value x_j		Uncertainty $u(x_j)$		Prob. Dist.	Sens. Coeff. c_i		$c_i u(x_j)$		ν
δK_A	0.0E+00	pulse/L	1.5E-04	pulse/L	t	1.0E+00	-	1.5E-04	pulse/L	4
δK_{B1}	0.0E+00	pulse/L	1.3E-04	pulse/L	rectangular	1.0E+00	-	1.3E-04	pulse/L	∞
δK_{B2}	0.0E+00	pulse/L	3.2E-04	pulse/L	rectangular	1.0E+00	-	3.2E-04	pulse/L	∞
δK_{B3}	0.0E+00	pulse/L	5.3E-04	pulse/L	rectangular	1.0E+00	-	5.3E-04	pulse/L	∞
δK_{B4}	0.0E+00	pulse/L	2.7E-04	pulse/L	rectangular	1.0E+00	-	2.7E-04	pulse/L	∞
δP_{DUT}	3.1E+04	pulse	4.1E-01	pulse	rectangular	6.3E-05	1/L	2.6E-05	pulse/L	∞
δV_{REF}	1.6E+04	L	4.7E+00	L	rectangular	-1.2E-04	pulse/L ²	-5.9E-04	pulse/L	∞
K_A	1.965 3	pulse/L						9.2E-04	pulse/L	6 308
$U(K)$								1.8E-03	pulse/L	

(c) 602.65 m³/h

Quantity X_j	Value x_j		Uncertainty $u(x_j)$		Prob. Dist.	Sens. Coeff. c_i		$c_i u(x_j)$		ν
δK_A	0.0E+00	pulse/L	1.9E-04	pulse/L	t	1.0E+00	-	1.9E-04	pulse/L	4
δK_{B1}	0.0E+00	pulse/L	1.7E-04	pulse/L	rectangular	1.0E+00	-	1.7E-04	pulse/L	∞
δK_{B2}	0.0E+00	pulse/L	3.9E-04	pulse/L	rectangular	1.0E+00	-	3.9E-04	pulse/L	∞
δK_{B3}	0.0E+00	pulse/L	5.6E-04	pulse/L	rectangular	1.0E+00	-	5.6E-04	pulse/L	∞
δK_{B4}	0.0E+00	pulse/L	2.7E-04	pulse/L	rectangular	1.0E+00	-	2.7E-04	pulse/L	∞
δP_{DUT}	2.1E+04	pulse	4.1E-01	pulse	rectangular	9.5E-05	1/L	3.9E-05	pulse/L	∞
δV_{REF}	1.1E+04	L	3.2E+00	L	rectangular	-1.9E-04	pulse/L ²	-5.9E-04	pulse/L	∞
K_A	1.964 1	pulse/L						9.7E-04	pulse/L	2 808
$U(K)$								1.9E-03	pulse/L	

(d) 301.79 m³/h

Quantity X_j	Value x_j		Uncertainty $u(x_j)$		Prob. Dist.	Sens. Coeff. c_i		$c_i u(x_j)$		ν
δK_A	0.0E+00	pulse/L	1.5E-04	pulse/L	t	1.0E+00	-	1.5E-04	pulse/L	4
δK_{B1}	0.0E+00	pulse/L	3.7E-05	pulse/L	rectangular	1.0E+00	-	3.7E-05	pulse/L	∞
δK_{B2}	0.0E+00	pulse/L	1.9E-04	pulse/L	rectangular	1.0E+00	-	1.9E-04	pulse/L	∞
δK_{B3}	0.0E+00	pulse/L	5.2E-04	pulse/L	rectangular	1.0E+00	-	5.2E-04	pulse/L	∞
δK_{B4}	0.0E+00	pulse/L	2.7E-04	pulse/L	rectangular	1.0E+00	-	2.7E-04	pulse/L	∞
δP_{DUT}	2.0E+04	pulse	4.1E-01	pulse	rectangular	9.7E-05	1/L	4.0E-05	pulse/L	∞
δV_{REF}	1.0E+04	L	3.1E+00	L	rectangular	-1.9E-04	pulse/L ²	-5.9E-04	pulse/L	∞
K_A	1.963 2	pulse/L						8.7E-04	pulse/L	4 426
$U(K)$								1.7E-03	pulse/L	

Table 9. Inconclusiveness analysis on the FM

q_{REF} [m ³ /h]	K_A [pulse/L]	u_{Base} [%]	u_{TS} [%]	u_{TS}/u_{Base}	$\sqrt{u_A^2 + u_{TS}^2}/u_{Base}$
1 201.44	1.964 8	0.030	0.022	0.74	0.75
902.05	1.965 3	0.030	0.035	1.17	1.20
602.65	1.964 1	0.030	0.038	1.28	1.32
301.79	1.963 2	0.030	0.032	1.06	1.09

3.2.7. Inconclusiveness test for K-factors

The type B uncertainty due to the FM (u_{TS}) is expressed as follows.

$$u_{TS} = \sqrt{c_{P_{DUT}}^2 u^2(\delta P_{DUT}) + u_{B1}^2 + u_{B2}^2 + u_{B3}^2 + u_{B4}^2} \quad [\text{pulse/L}] \quad (16)$$

The base uncertainty (u_{Base}) is converted from [L] to [pulse/L] as follows.

$$u_{Base} = c_{V_{REF}} u(\delta V_{REF}) \quad [\text{pulse/L}] \quad (17)$$

It is noticeable that u_A is not needed to calculate either u_{TS} or u_{Base} . It is because u_A is influenced by comparison calibration between the FM and the gravimetric water flow measurement standard. This means that covariance between u_{TS} and u_{Base} must be separated from u_A . Then, u_A can be partitioned into a part belonged to u_{TS} and the other part belonged to u_{Base} . Even though u_A is incorporated into u_A , the ratio of $\sqrt{u_A^2 + u_{TS}^2}$ to u_{Base} becomes a value less than 2 [11]. This indicates that the inconclusiveness analysis satisfies the measurement equivalence between NMIJ, AIST and KRISS.

The inconclusiveness test can be performed by dividing u_{TS} with u_{Base} as shown in Table 9. u_{TS}/u_{Base} showed its maximum value of 1.28 at 602.65 m³/h. Since $u_{TS}/u_{Base} < 2$ at each flow rate, it is convinced that the experimental results should be conclusive [11].

3.3. Definition of E_n

Number of equivalence between NMIJ, AIST and KRISS is calculated as follows.

$$E_n = \frac{|K_{NMIJ} - K_{KRISS}|}{\sqrt{U^2(K_{NMIJ}) + U^2(K_{KRISS})}} \quad (18)$$

Here, E_n is the number of equivalence, K_{NMIJ} is the K-factor measured by NMIJ, AIST

[pulse/L], K_{KRIS} is the K-factor measured by KRIS [pulse/L], $U(K_{\text{NMIJ}})$ is the measurement uncertainty of K_{NMIJ} by NMIJ, AIST [pulse/L], and $U(K_{\text{KRIS}})$ is the measurement uncertainty of K_{KRIS} by K_{KRIS} [pulse/L]. It is noticeable that both K-factors were corrected by Eq. (5) with the reference temperature of $T_{@20^{\circ}\text{C}}$. E_n was evaluated at [300, 600, 900, 1 200] m³/h, separately. If $E_n \leq 1$, the measurement equivalence between NMIJ, AIST and KRIS is established.

4. Test Results

4.1. Test results with the FC according to Configuration #2

4.1.1. First experimental results between dataset #1 and dataset #2

Test results according to configuration #2 were summarized in Table 10 and Figs. 6 and 7. Before correcting the influence of temperature change, E_n was distributed between 0.01 and 0.99 in Fig. 6. E_n could be evaluated at $T_{@20^{\circ}\text{C}}$ by applying Eq. (5) such that E_n was distributed between 0.06 and 0.94 as shown in Table 10 and Fig. 6.

KRISS showed a characteristic curve of the FM, which was cambered upward at around 900 m³/h, while NMIJ, AIST showed a straight line as the characteristic curve in Fig. 7. The cambered characteristic curve at KRISS could be because of the flow characteristics of the flow diverter attached to the gravimetric water flow measurement standard.

Table 10. Number of equivalence between dataset #1 (KRISS) and #2 (NMIJ, AIST)

No.	q_{REF} m ³ /h	NMIJ, AIST			KRISS			E_n
		U_{CMC} %	K_{NMIJ} pulse/L	$U(K_{\text{NMIJ}})$ pulse/L	U_{CMC} %	K_{KRISS} pulse/L	$U(K_{\text{KRISS}})$ pulse/L	
1	1 200	0.06	1.965 01	0.001 179	0.06	1.964 91	0.001 191	0.06
2	900	0.06	1.964 01	0.001 178	0.06	1.965 38	0.001 236	0.80
3	600	0.06	1.963 11	0.001 178	0.06	1.964 20	0.001 308	0.62
4	300	0.06	1.961 67	0.001 177	0.06	1.963 29	0.001 260	0.94

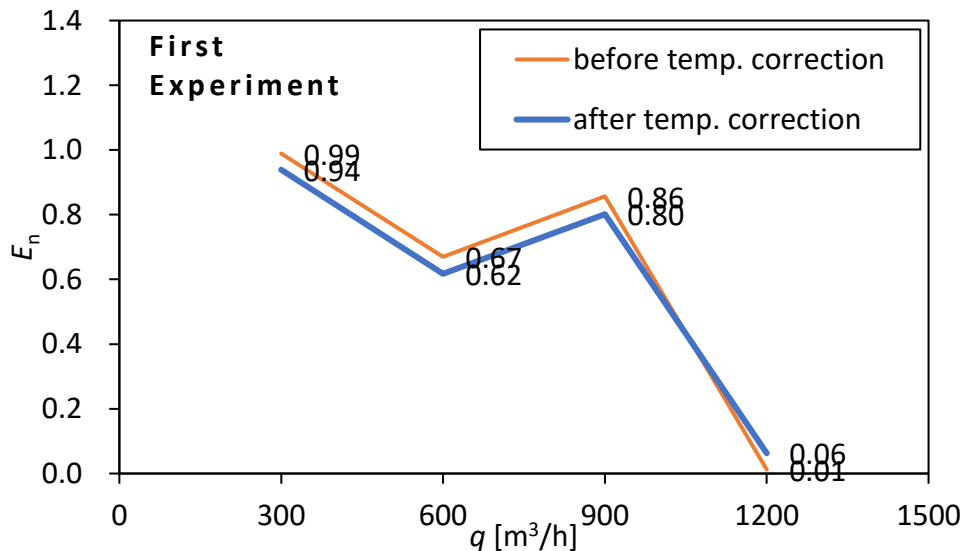


Figure 6. Number of equivalence between dataset #1 (KRISS) and #2 (NMIJ, AIST)

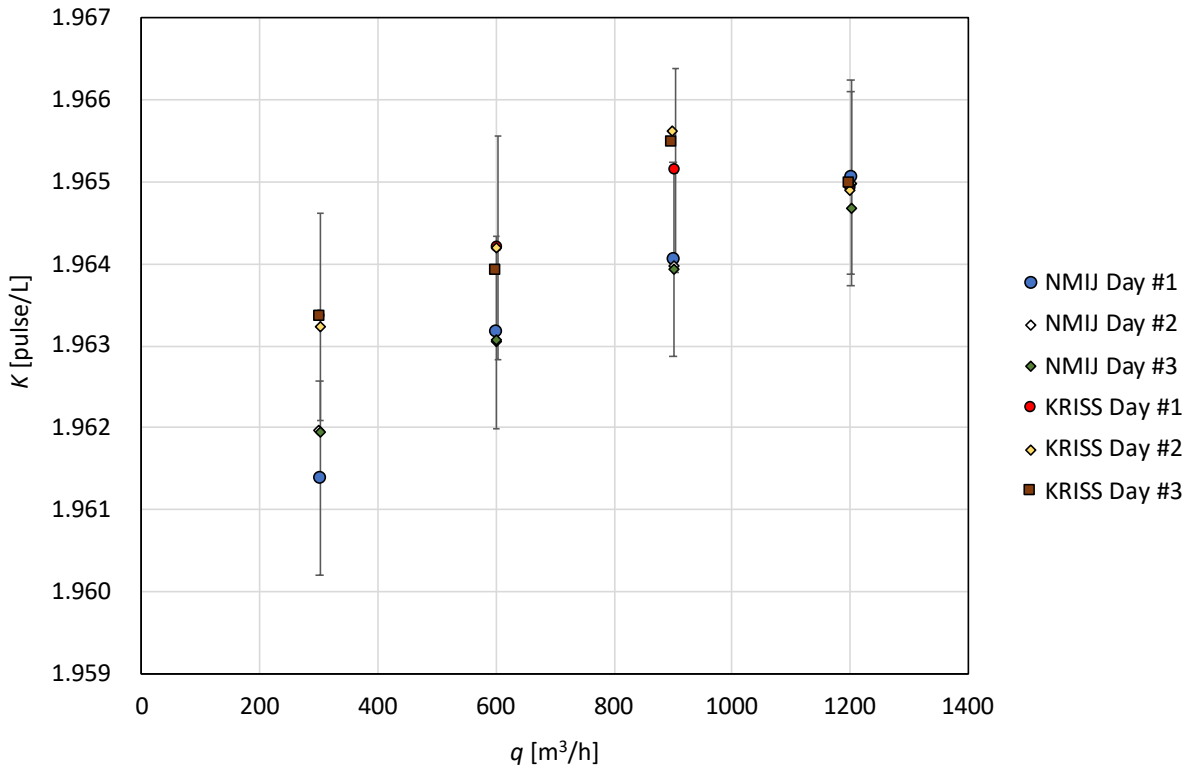


Figure 7. Test results between dataset #1 (KRISS) and #2 (NMIJ, AIST)

Table 11. Number of equivalence between dataset #2 (NMIJ, AIST) and #3 (KRISS)

No.	q_{REF} m ³ /h	NMIJ, AIST			KRISS			E_n
		U_{CMC} %	K_{NMIJ} pulse/L	$U(K_{NMIJ})$ pulse/L	U_{CMC} %	K_{KRISS} pulse/L	$U(K_{KRISS})$ pulse/L	
1	1 200	0.06	1.965 01	0.001 179	0.06	1.964 31	0.001 188	0.42
2	900	0.06	1.964 01	0.001 178	0.06	1.963 99	0.001 210	0.01
3	600	0.06	1.963 11	0.001 178	0.06	1.963 35	0.001 188	0.14
4	300	0.06	1.961 67	0.001 177	0.06	1.963 00	0.001 294	0.76

4.1.2. Second experimental results between dataset #2 and dataset #3

Test results according to configuration #2 were summarized again in Table 11 and Figs. 8 and 9. Before correcting the influence of temperature change, E_n was distributed between 0.08 and 0.84 in Fig. 8. E_n could be evaluated at $T_{@20^{\circ}\text{C}}$ by applying Eq. (5) such that E_n was distributed between 0.01 and 0.76 as shown in Table 11 and Fig. 9.

KRISS showed a slightly better characteristic curve of the FM, which was still cambered upward at around 900 m³/h. It could be partly because of improved bearing resistance to support a rotor in the FM. It was also because of uncertain flow disturbances which were suppressed by the FC. In both experimental results, the measurement equivalence between NMIJ, AIST and KRISS was established.

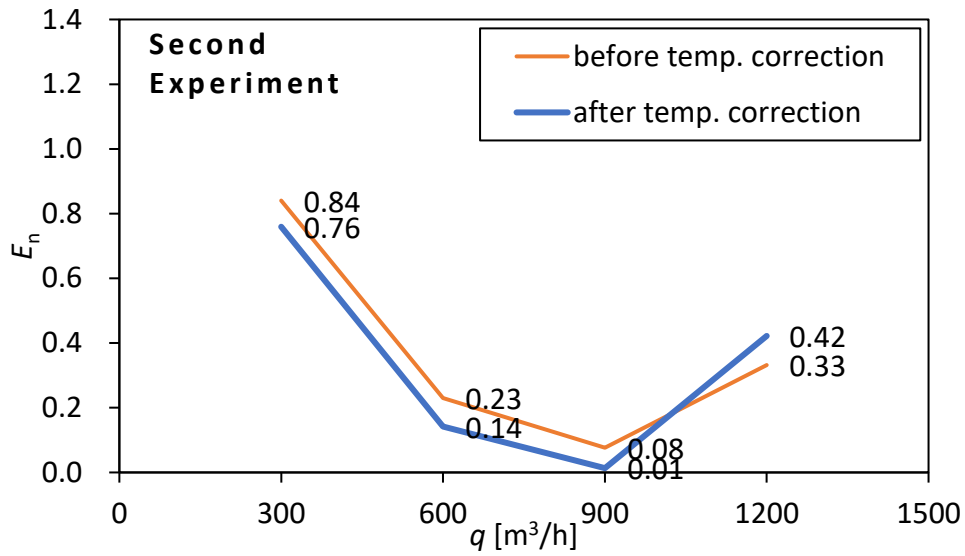


Figure 8. Number of equivalence between dataset #2 (NMIJ, AIST) and #3 (KRISS)

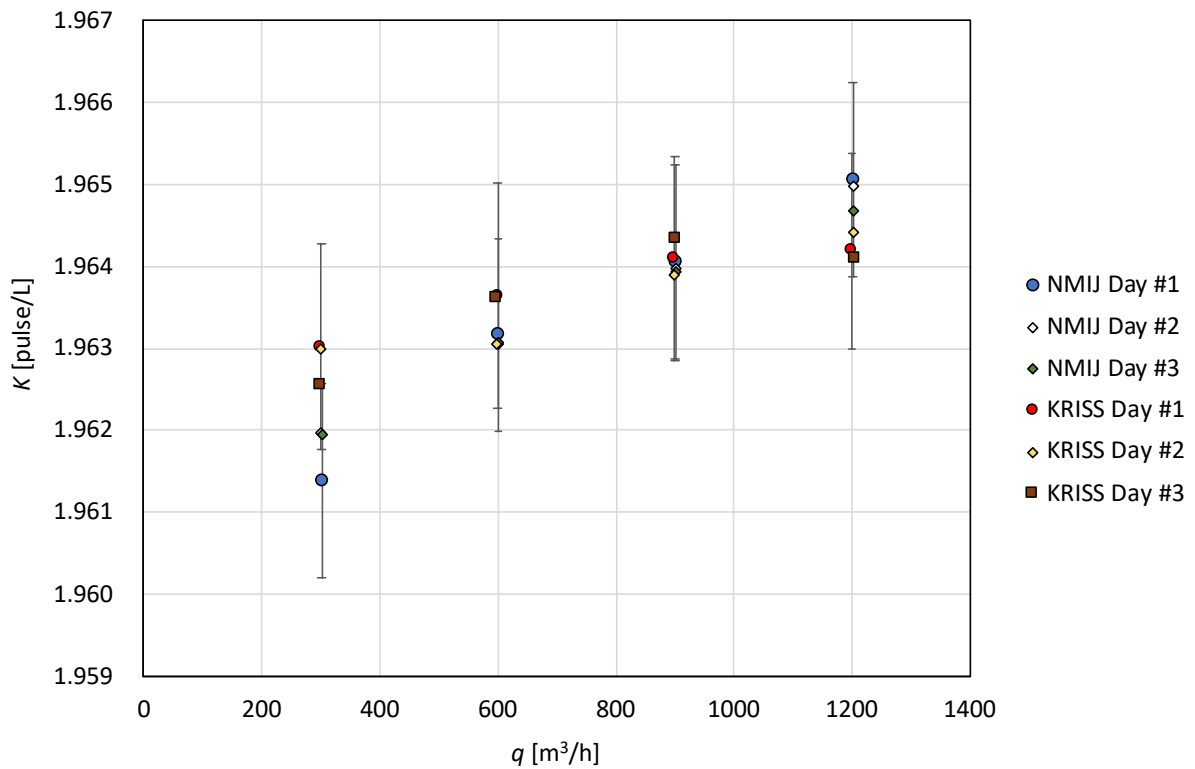


Figure 9. Test results between dataset #2 (NMIJ, AIST) and #3 (KRISS)

4.2. Test results without the FC according to Configurations #1 and #3

Test results according to configurations #1 and #3 were summarized again in Table 12 and Figs. 10 and 11. Before correcting the influence of temperature change, E_n was distributed between 0.14 and 0.49 in Fig. 10. E_n could be evaluated at $T_{@20^{\circ}\text{C}}$ by applying Eq. (5) such that E_n was distributed between 0.08 and 0.37 in Table 12 and Fig. 11.

NMIJ, AIST and KRISS gave much better agreements without the FC than the experimental results with the FC. One possible explanation is to say that the flow disturbances were effectively removed by configuration #3 at KRISS. Considering the FC and the FS, the FC required longer straight pipe length upstream of the FM than the FS required.

Table 12. Number of equivalence between configuration #1 (NMIJ, AIST) and #3 (KRISS)

No.	q_{REF} m ³ /h	NMIJ, AIST			KRISS			E_n
		U_{CMC} %	K_{NMIJ} pulse/L	$U(K_{NMIJ})$ pulse/L	U_{CMC} %	K_{KRISS} pulse/L	$U(K_{KRISS})$ pulse/L	
1	1 200	0.06	1.962 99	0.001 178	0.06	1.962 58	0.001 202	0.24
2	900	0.06	1.962 07	0.001 177	0.06	1.962 52	0.001 181	0.27
3	600	0.06	1.961 41	0.001 177	0.06	1.962 04	0.001 188	0.37
4	300	0.06	1.960 94	0.001 177	0.06	1.961 09	0.001 221	0.08

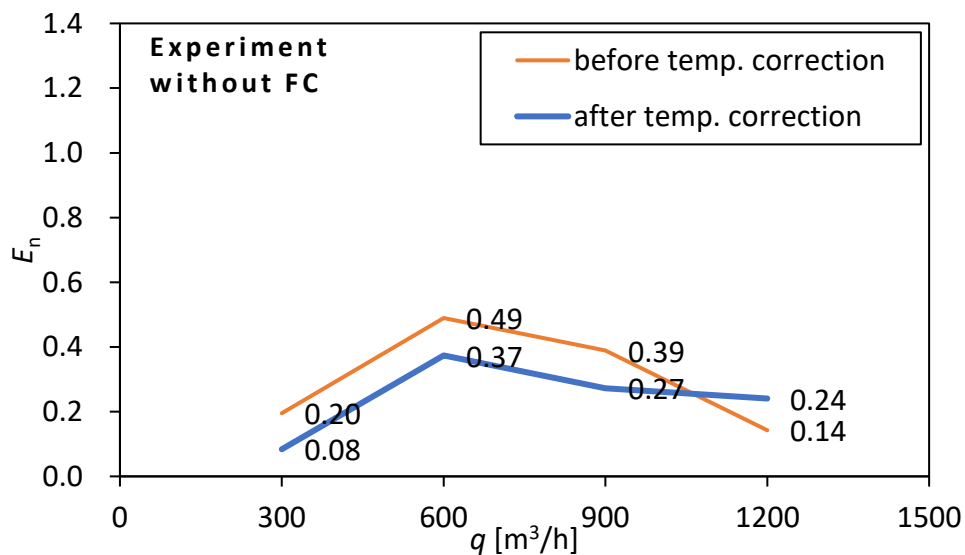


Figure 10. Number of equivalence between configuration #1 (NMIJ, AIST) and #3 (KRISS)

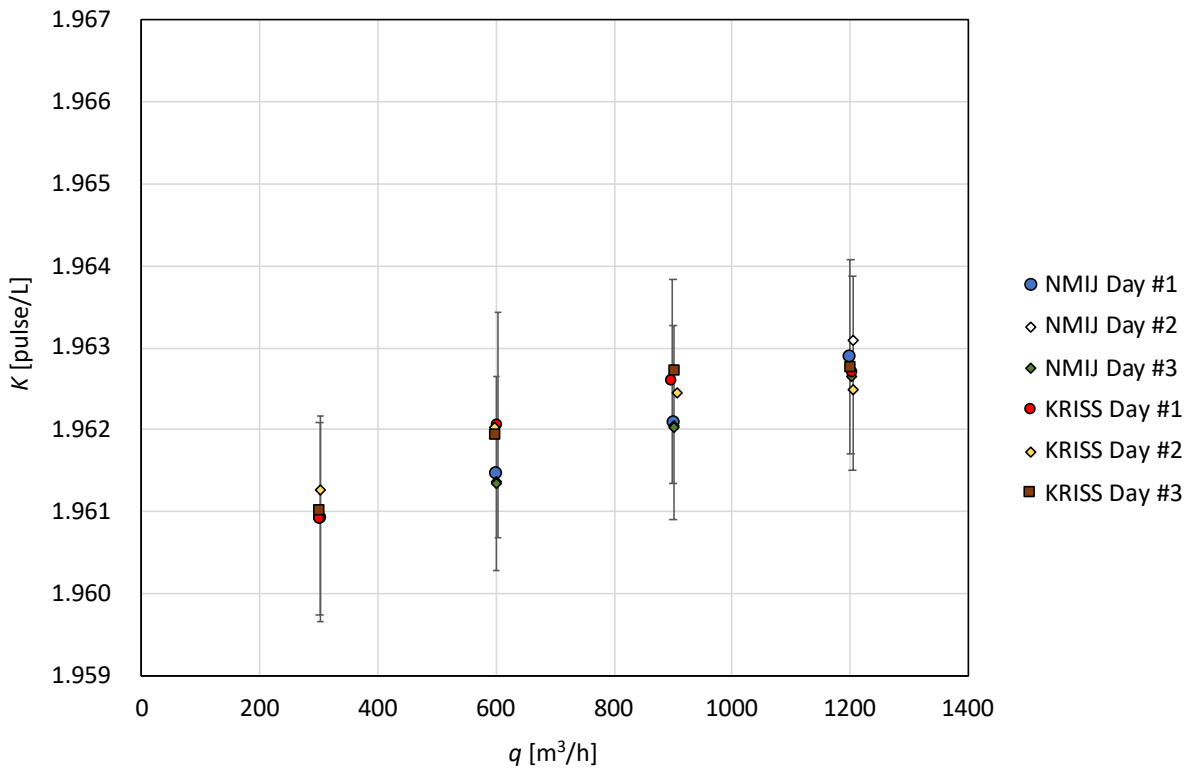


Figure 11. Test results between configuration #1 (NMIJ, AIST) and #3 (KRISS)

5. Conclusions

A supplementary inter-comparison, named as APMP.M.FF-S1, was performed to find an evidence for measurement equivalence between NMIJ, AIST and KRISS. The APMP.M.FF-S1 was a spin-off inter-comparison from the CCM.FF-K1 in that its flow range was changed from [30 to 200] m³/h (CCM.FF-K1) to [300 to 1 200] m³/h (APMP.M.FF-S1). A turbine flow meter with a flow conditioner was employed as the transfer standard in the APMP.M.FF-S1. Relationship to the CMC's tables were summarized in Table 13.

An inflow condition upstream of the turbine flow meter was critical in establishing the measurement equivalence between NMIJ, AIST and KRISS. The flow conditioner played a role as the starting point of measuring upstream pipe length for flow measurement. Otherwise, each laboratory would have different starting points of measuring upstream pipe length. NMIJ, AIST had a long straight upstream pipeline more than 100*D* (*D* as the pipe diameter) while KRISS had a short straight upstream pipeline less than 40*D*. Instead, KRISS installed a tube-bundle flow straightener according to ISO 5167-1.

The number of equivalence was proven to be less than 1 at [300, 600, 900, 1 200] m³/h. This means that the measurement equivalence between NMIJ, AIST and KRISS has been established. Thermal expansion of the turbine flow meter, which was made of SUS 304, was considered for correcting the K-factor by turbine flow metering. Temperature correction gave better measurement equivalence between NMIJ, AIST and KRISS than the cases without temperature correction.

Inconclusiveness test for turbine flow metering was investigated by classifying the uncertainty factors into those from the turbine flow meter and those from the gravimetric water flow measurement standard. The inconclusiveness index, which was the ratio of the uncertainty by transfer standard to the base uncertainty, was less than 2. This indicated that the test results were conclusive.

The above results indicated measurement equivalence between NMIJ, AIST and KRISS in the flow range of [83.3 to 333.3] kg/s (that is, [300 to 1 200] t/h). The results will be used for supporting a new calibration service by KRISS in the next peer review, which is scheduled in 2022.

Table 13. Relationship to the CMC's tables

NMI / Country	Flow range declared in CMC's tables	Expanded uncertainty declared in CMC's tables ^{*)}	Result
NMIJ, AIST / Japan	[13.9 to 833] kg/s	0.06 %	In accordance ^{*)}
KRISS / Korea	[11 to 110] kg/s	0.08 %	For further support to achieve ^{**)} [83.3 to 333.3] kg/s @ 0.06 %

*) All the laboratories, that have CMC's published in the KCDB, represented uncertainty values in accordance with their CMC claims.

**) If the country has not yet CMC tables, the results will be used for supporting a new service in the next peer review.

Acknowledgements

APMP.M.FF-S1 SC was financially supported by Korea Research Institute of Standards and Science (grant no. 20011027) in South Korea. One of the authors (Sejong Chun) is grateful to Dr. Woong Kang and Dr. Takashi Shimada for establishing this supplementary comparison. Sejong Chun is also grateful to Mr. Byung-Ro Yoon for conducting experiments for turbine flow meter testing.

References

- [1] Paik J S, Lee K-B, Lau P, Engel R, Loza A, Terao Y and Reader-Harris M 2007 CCM.FF-K1 for Water Flow - Final Report.
- [2] Cordova L, Furuichi N and Lederer T 2015 Qualification of an ultrasonic flow meter as a transfer standard for measurements at Reynolds numbers up to 4×10^6 between NMIJ and PTB *Flow Measurement and Instrumentation* **45** 28-42
- [3] ISO 2017 Liquid hydrocarbons - Volumetric measurement by turbine flowmeter. (Geneva, Swiss: International Organization for Standardization)
- [4] CIPM 2011 CIPM MRA Guidelines for Authorship of Key, Supplementary and Pilot Study Comparison Reports. (Paris, France: Bureau International de Poids et Mesures)
- [5] CIPM 2016 Measurement comparisons in the CIPM MRA. (Paris, France: Bureau International de Poids et Mesures)
- [6] ISO 2003 Measurement of fluid flow by means of pressure differential devices inserted in circular cross-section conduits running full. In: *Part 1: General principles and requirements*, (Geneva, Swiss: International Organization for Standardization)
- [7] Corruccini R J and Gniewek J J 1961 Thermal expansion of technical solids at low temperatures - A compilation from the literature. (Washington D.C., USA: National Bureau of Standards)
- [8] ISO 2008 Uncertainty of measurement - Part 3: Guide to the expression of uncertainty in measurement (GUM:1995) (ISO/IEC Guide 98-3:2008). (Geneva, Swiss: International Organization for Standardization)
- [9] EA 2013 Evaluation of the uncertainty of measurement in calibration (EA-4/02 M:2013). (Paris, France: European Accreditation)
- [10] Lee S H, Park S, Lee J and Kang W 2019 Practical methodology for in situ measurement of micro flow rates using laser diode absorption sensors *Metrologia* **56**
- [11] Wright J, Toman B, Mickan B, Wubbeler G, Bodnar O and Elster C 2016 Transfer Standard Uncertainty Can Cause Inconclusive Inter-Laboratory Comparisons *Metrologia* **53**

Appendix

A.1. Test results by NMIJ, AIST (Dataset #2, September 11 ~ 17, 2019)

1) Day 1

No.	q_{REF} [m ³ /h]	P_{DUT} [pulse]	V_{REF} [L]	K_A [pulse/L]	T °C		P kPa		$U(K)$ [m ³ /h]
					up	down	up	down	
1	1 202	84 499.4	43 004.4	1.964 89		25.49		106.1	0.001 179
2	901	83 972.4	42 758.3	1.963 88		25.67		163.9	0.001 178
3	600	84 056.8	42 820.9	1.962 98		25.81		205.1	0.001 178
4	301	83 713.4	42 684.8	1.961 20		25.89		228.6	0.001 177

2) Day 2

No.	q_{REF} [m ³ /h]	P_{DUT} [pulse]	V_{REF} [L]	K_A [pulse/L]	T °C		P kPa		$U(K)$ [m ³ /h]
					up	down	up	down	
1	1 201	84 103.6	42 804.8	1.964 80		25.31		102.6	0.001 179
2	901	84 200.0	42 875.6	1.963 81		25.40		160.2	0.001 178
3	601	84 039.6	42 814.1	1.962 89		25.46		201.4	0.001 178
4	301	84 617.4	42 622.8	1.961 79		25.51		226.9	0.001 177

3) Day 3

No.	q_{REF} [m ³ /h]	P_{DUT} [pulse]	V_{REF} [L]	K_A [pulse/L]	T °C		P kPa		$U(K)$ [m ³ /h]
					up	down	up	down	
1	1 201	83 941.6	42 727.6	1.964 56		23.52		106.9	0.001 179
2	901	84 019.6	42 783.3	1.963 83		23.53		163.9	0.001 178
3	600	84 113.4	42 850.2	1.962 96		23.53		205.3	0.001 178
4	302	83 767.6	42 698.3	1.961 84		23.51		230.5	0.001 177

A.2. Test results by NMIJ, AIST (Configuration #1, September 11 ~ 17, 2019)

1) Day 1

No.	q_{REF} [m ³ /h]	P_{DUT} [pulse]	V_{REF} [L]	K_A [pulse/L]	T °C		P kPa		$U(K)$ [m ³ /h]
					up	down	up	down	
1	1 201	84 124.6	42 859.3	1.962 79		23.20		142.4	0.001 178
2	901	83 837.0	42 730.6	1.961 99		23.24		184.3	0.001 177
3	601	84 055.4	42 855.4	1.961 37		23.27		214.4	0.001 177
4	301	83 641.2	42 656.2	1.960 82		23.28		232.8	0.001 176

2) Day 2

No.	q_{REF} [m ³ /h]	P_{DUT} [pulse]	V_{REF} [L]	K_A [pulse/L]	T °C		P kPa		$U(K)$ [m ³ /h]
					up	down	up	down	
1	1 205	84 102.4	42 843.4	1.963 00		22.74		139.0	0.001 178
2	902	83 941.4	42 784.4	1.961 96		22.86		180.7	0.001 177
3	600	83 904.4	42 780.5	1.961 27		22.99		210.9	0.001 177
4	300	83 645.4	42 657.0	1.960 87		23.11		229.5	0.001 177

3) Day 3

No.	q_{REF} [m ³ /h]	P_{DUT} [pulse]	V_{REF} [L]	K_A [pulse/L]	T °C		P kPa		$U(K)$ [m ³ /h]
					up	down	up	down	
1	1 202	84 028.6	42 815.2	1.962 57		22.22		142.3	0.001 178
2	901	84 015.4	42 821.9	1.961 95		22.35		184.5	0.001 177
3	602	83 660.8	42 656.2	1.961 27		22.50		214.5	0.001 177
4	302	83 628.4	42 649.1	1.960 84		22.67		233.0	0.001 177

A.3. Test results by KRISS (Dataset #1, July 8 ~ 12, 2019)

1) Day 1

No.	q_{REF} [m ³ /h]	P_{DUT} [pulse]	V_{REF} [L]	K_A [pulse/L]	T °C		P kPa		$U(K)$ [m ³ /h]
					up	down	up	down	
1	1 202	41 330.0	21 034.7	1.964 85	22.18	22.27	201.4	82.7	0.001 189
2	904	31 089.6	15 821.1	1.965 07	22.32	22.38	203.7	134.3	0.001 245
3	604	20 655.6	10 516.5	1.964 12	22.52	22.58	205.6	172.3	0.001 371
4	302	20 195.4	10 286.6	1.963 26	22.71	22.75	205.9	194.9	0.001 257

2) Day 2

No.	q_{REF} [m ³ /h]	P_{DUT} [pulse]	V_{REF} [L]	K_A [pulse/L]	T °C		P kPa		$U(K)$ [m ³ /h]
					up	down	up	down	
1	1 201	41 300.0	21 019.8	1.964 81	22.47	22.56	201.3	82.6	0.001 193
2	900	31 047.0	15 795.7	1.965 53	22.64	22.70	203.8	134.9	0.001 228
3	602	20 722.6	10 550.7	1.964 10	22.90	22.95	205.4	172.0	0.001 242
4	302	20 204.8	10 292.1	1.963 14	23.10	23.15	206.3	195.9	0.001 263

3) Day 3

No.	q_{REF} [m ³ /h]	P_{DUT} [pulse]	V_{REF} [L]	K_A [pulse/L]	T °C		P kPa		$U(K)$ [m ³ /h]
					up	down	up	down	
1	1 200	41 330.8	21 035.0	1.964 86	23.51	23.60	201.1	82.7	0.001 192
2	900	31 019.2	15 783.0	1.965 36	23.65	23.72	203.6	134.8	0.001 195
3	601	20 652.0	10 516.4	1.963 80	23.80	23.85	205.2	172.2	0.001 264
4	301	20 200.6	10 289.5	1.963 22	23.96	24.00	206.7	194.3	0.001 225

A.4. Test results by KRISS (Dataset #3, November 24 ~ 29, 2019)

1) Day 1

No.	q_{REF} [m ³ /h]	P_{DUT} [pulse]	V_{REF} [L]	K_A [pulse/L]	T °C		P kPa		$U(K)$ [m ³ /h]
					up	down	up	down	
1	1 200	41 313.4	21 033.5	1.964 17	20.49	20.58	201.4	90.1	0.001 188
2	900	31 125.6	15 847.5	1.964 07	20.66	20.73	203.7	139.1	0.001 181
3	599	20 882.4	10 634.7	1.963 61	20.79	20.84	205.3	174.4	0.001 184
4	301	20 176.2	10 278.3	1.962 99	20.94	20.98	206.9	194.1	0.001 309

2) Day 2

No.	q_{REF} [m ³ /h]	P_{DUT} [pulse]	V_{REF} [L]	K_A [pulse/L]	T °C		P kPa		$U(K)$ [m ³ /h]
					up	down	up	down	
1	1 203	41 392.0	21 071.0	1.964 40	20.62	20.71	201.2	89.6	0.001 187
2	900	31 029.8	15 800.4	1.963 87	20.75	20.82	203.7	138.9	0.001 239
3	599	20 644.2	10 516.5	1.963 02	21.03	21.09	205.3	174.2	0.001 193
4	301	20 197.2	10 289.2	1.962 94	21.27	21.32	206.6	195.6	0.001 279

3) Day 3

No.	q_{REF} [m ³ /h]	P_{DUT} [pulse]	V_{REF} [L]	K_A [pulse/L]	T °C		P kPa		$U(K)$ [m ³ /h]
					up	down	up	down	
1	1 204	41 267.0	21 009.7	1.964 19	16.83	16.92	201.5	89.4	0.001 186
2	903	30 972.2	15 766.5	1.964 43	16.98	17.04	203.9	138.4	0.001 215
3	599	20 662.2	10 522.1	1.963 70	17.13	17.19	205.6	174.4	0.001 224
4	301	20 178.6	10 281.5	1.962 62	17.38	17.42	206.6	195.7	0.001 217

A.5. Test results by KRISS (Configuration #3, November 24 ~ 29, 2019)

1) Day 1

No.	q_{REF} [m ³ /h]	P_{DUT} [pulse]	V_{REF} [L]	K_A [pulse/L]	T °C		P kPa		$U(K)$ [m ³ /h]
					up	down	up	down	
1	1 204	41 294.8	21 038.4	1.962 83	15.41	15.50	201.5	117.2	0.001 210
2	900	31 066.0	15 827.9	1.962 73	15.66	15.72	204.0	154.3	0.001 178
3	603	20 784.6	10 592.6	1.962 18	15.81	15.86	205.6	181.1	0.001 188
4	302	20 151.2	10 275.8	1.961 04	15.98	16.03	206.9	197.8	0.001 192

2) Day 2

No.	q_{REF} [m ³ /h]	P_{DUT} [pulse]	V_{REF} [L]	K_A [pulse/L]	T °C		P kPa		$U(K)$ [m ³ /h]
					up	down	up	down	
1	1 205	41 232.0	21 009.4	1.962 55	17.71	17.79	201.6	117.3	0.001 195
2	907	31 158.0	15 876.6	1.962 51	17.91	17.98	203.9	153.8	0.001 185
3	598	20 750.6	10 575.8	1.962 08	18.05	18.11	205.7	181.2	0.001 187
4	302	20 160.8	10 279.2	1.961 32	18.20	18.25	207.0	196.8	0.001 250

3) Day 3

No.	q_{REF} [m ³ /h]	P_{DUT} [pulse]	V_{REF} [L]	K_A [pulse/L]	T °C		P kPa		$U(K)$ [m ³ /h]
					up	down	up	down	
1	1 204	41 275.8	21 028.5	1.962 85	17.16	17.24	201.5	116.8	0.001 190
2	903	30 988.4	15 788.0	1.962 78	17.41	17.47	203.8	154.0	0.001 192
3	602	20 627.2	10 513.4	1.961 99	17.95	18.01	205.5	180.8	0.001 214
4	303	20 189.6	10 295.2	1.961 06	18.11	18.16	206.4	197.2	0.001 237